
SLaNC: Static LayerNorm Calibration

Anonymous Author(s)

Affiliation

Address

email

Abstract

1 The ever increasing sizes of Large Language Models (LLMs) beyond hundreds of
2 billions of parameters have generated enormous pressure on the manufacturers of
3 dedicated hardware accelerators and made the innovative design of the latter one
4 of the most rapidly expanding fields of the AI industry. Various approaches have
5 been explored to enable efficient and accurate processing of LLMs on the avail-
6 able accelerators given their computational and storage limitations. Among these,
7 various quantization techniques have become the main focus of the community
8 as a means of reducing the compute, communication and storage requirements.
9 Quantization to lower precision formats naturally poses a number of challenges
10 caused by the limited range of the available value representations. When it comes
11 to processing the popular Transformer models on hardware, one of the main is-
12 sues becomes calculation of the LayerNorm simply because accumulation of the
13 variance requires a much wider dynamic range than the hardware enables. In
14 this article, we address this matter and propose a computationally-efficient scaling
15 technique that can be easily applied to Transformer models during inference. Our
16 method suggests a straightforward way of scaling the LayerNorm inputs based on
17 the static weights of the immediately preceding linear layers. The scaling factors
18 are computed offline, based solely on the linear layer weights, hence no latency
19 or computational overhead is added during inference. Most importantly, our tech-
20 nique ensures that no numerical issues such as overflow or underflow could happen
21 during the compute. This approach offers smooth, accurate and resource-effective
22 inference across a wide range of hardware architectures. The article provides the-
23oretical justification as well as supporting numerical simulations.

24 1 Introduction

25 Large Language Models (LLMs) based on Transformers [1] have recently become the dominant
26 Deep Neural Network (DNN) architecture due to their unprecedented performance results in all
27 language modeling [2, 3], text processing [4], image and video generation [5], and many other
28 tasks. However, this success comes at a cost of enormous volumes of compute, storage, and data
29 transfer. A whole new industry of dedicated hardware accelerators has emerged in the last few years
30 to accommodate the needs of LLM training and inference [6, 7]. Another major initiative targeted at
31 making the inference feasible and sustainable involves the development of lower precision formats
32 [8, 9, 10], efficient quantization techniques [11], algorithmic solutions [12], accurate approximations
33 [13], and other software optimizations [14, 15].

34 Efficient quantization techniques such as GPTQ [16], AWQ [17], SmoothQuant [18], KVQuant [19],
35 K-sort [20], and numerous others enable storing and processing of LLMs in low-precision formats.
36 Often, that would involve training the model in FP32 format and casting it to 4, 8 or 16-bit precision
37 formats before deployment onto inference hardware [11, 21, 20]. The most popular approach is to

38 compress the static weights to 4 or 8-bit integers or floats and reduce the activations to FP16 or BF16
 39 [22]. In this paper, we focus on the wide family of accelerators operating on FP16 activations for
 40 their popularity [23, 24] and specifically for the relatively narrow dynamic range (the range of repre-
 41 sentable numbers) of FP16 which might pose significant computational challenges. The most critical
 42 manifestation of this problem occurs during the LayerNorm computation. Importantly, inclusion of
 43 dozens or even hundreds of LayerNorm operators in current Transformers is unavoidable since they
 44 prevent the gradients from exploding or decaying during training [25]. At inference, though, pro-
 45 cessing LayerNorms on accelerators is extremely challenging because they require accumulation of
 46 squares of the inputs for the sake of variance (and norm) calculation [26]. Accumulation of such a
 47 large number of positive values in FP16 is almost surely bound to overflow.

48 In this work, we address this problem and propose an efficient, theoretically justified, and easy to
 49 implement scaling technique that leads to complete elimination of the FP16 overflow (or underflow)
 50 issue in LayerNorms. First, note that scaling of the LayerNorm input does not affect the output due
 51 to the homogeneity of the normalization operation but can very significantly shift the range of the
 52 accumulated numbers in the denominator computation. Based on this observation, we developed the
 53 SLaNC (Static LayerNorm Calibration) method which provides succinct closed formulae for scaling
 54 the inputs of all LayerNorms of any Transformer. Importantly, the SLaNC scales are computed
 55 solely based on the static weights of the preceding liner layers, and can be therefore computed
 56 offline without impacting the inference runtime. The formulae suggested by SLaNC are theoretically
 57 justified by derivations and detailed explanations and only involve norms of static weight matrices
 58 that can be directly and precisely computed using standard software.

59 The rest of the article is organized as follows. First, we outline the notation, then in Section 2 we
 60 formulate the numerical problem caused by the LayerNorm computation in FP16. Section 3 presents
 61 the SLaNC technique together with its theoretical justification. Supporting numerical simulation on
 62 the Llama family of LLMs are demonstrated in Section 4. The concluding remarks can be found in
 63 Section 5.

64 **Notation.** The following notation is used in the article. Matrices are denoted by capital bold letters
 65 \mathbf{M} and vectors by lower case bold \mathbf{v} . The operator product of matrices \mathbf{A} and \mathbf{B} of appropriate sizes
 66 is written as $\mathbf{A} \cdot \mathbf{B}$ or \mathbf{AB} , while their element-wise product would be denoted by $\mathbf{A} \odot \mathbf{B}$. For matrix
 67 \mathbf{M} , we write $\|\mathbf{M}\|_F$ for its Frobenius norm and $\|\mathbf{M}\|$ for its spectral norm; for vector \mathbf{v} , by $\|\mathbf{v}\|$ we
 68 denote its Euclidean norm. Given vector \mathbf{m} , we denote by $\mathbf{M} = \text{diag}(\mathbf{m})$ the diagonal matrix with
 69 elements of \mathbf{m} on the main diagonal.

70 2 Problem Formulation

71 Quantization of an LLM to a low-precision format (e.g., 4, 8 or 16-bit) can lead to a significant
 72 degradation of the output quality, and thus has to be applied together with some advanced technique
 73 capable of restoring the accuracy [16, 17, 18, 19, 20, 27, 28]. However, an even bigger challenge
 74 caused by casting models into low-precision formats is the limited dynamic range of such formats,
 75 which can completely ruin the compute flow if applied blindly. The most prominent example is the
 76 computation of LayerNorm, which becomes impossible on FP16 accelerators due to the unavoidable
 77 overflows and underflows as demonstrated next.

78 2.1 LayerNorm Compute

79 Layer Normalization (LayerNorm) has become one of the most ubiquitous non-linear operations in
 80 modern DNNs since it prevents the gradients from decaying or exploding during training. Extensive
 81 literature has demonstrated that the current DNN architectures cannot be practically trained without
 82 frequent normalization of hidden states [29, 30, 31]. State of the art Transformer models include
 83 dozens or even hundreds of LayerNorm operators which are introduced to facilitate training but
 84 make inference troublesome due to the numerical problems introduced by the computation of their
 85 denominators.

86 Given a row input $\mathbf{x} \in \mathbb{R}^d$ and fixed parameters $\gamma, \beta \in \mathbb{R}^d$, the LayerNorm output reads as

$$\mathbf{y}(\mathbf{x}) = \left(\frac{\mathbf{x} - \mu \mathbf{1}}{\sigma} \right) * \gamma + \beta = \left(\frac{\mathbf{x} - \mu \mathbf{1}}{\sigma} \right) \mathbf{\Gamma} + \beta \in \mathbb{R}^d, \quad (1)$$

87 where $\mathbf{1} \in \mathbb{R}^d$ is the vector of ones, $\mathbf{\Gamma} = \text{diag}(\gamma)$, and

$$\mu = \frac{1}{d} \sum_{i=1}^d x_i, \quad \text{and} \quad \sigma = \sqrt{\frac{1}{d} \sum_{i=1}^d (x_i - \mu)^2} = \sqrt{\frac{1}{d} \sum_{i=1}^d x_i^2 - \mu^2}. \quad (2)$$

88 As Eq. 2 suggests, the standard way of computing σ
 89 requires summing up the squares of the input vector elements.
 90 Depending on the range of these elements, such accumu-
 91 lation can easily lead to an overflow or underflow when
 92 performed in FP16 or FP8 formats. It is important to note
 93 that the majority of the available LLM accelerators process
 94 non-linear operations exclusively in FP16 format [32, 33].
 95 While some accelerators do support FP32 accumulation in
 96 non-linear modules, this option often comes at a high la-
 97 tency increase making FP32 regime impractical. Fig. 3a and
 98 Fig. 3c show the typical distributions of the sum of squares
 99 from Eq. 2 in one of the layers of Llama-2. We observe that
 100 in too many cases the resulting values exceed the range of
 101 FP16, leading to invalid inference.

102 Note also that the Transformer architecture comes in two
 103 flavors based on the location of the residual branch-out. It
 104 can take off before the LayerNorm (pre-LN residual) or af-
 105 ter (post-LN residual), Fig. 1. Originally, the post-LN op-
 106 tion was suggested [1] but later the other one became quite
 107 popular since it was observed to speed-up the training [34].
 108 To be specific and for lack of space below we focus on the
 109 post-LN design, however, we emphasize that the deriva-
 110 tions and conclusions equally apply to the pre-LN one.

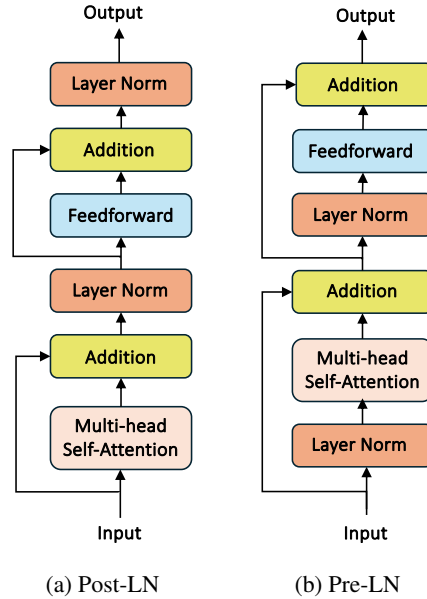


Figure 1: Residual branching options.

111 3 LayerNorm Scaling

112 3.1 Dynamic Model Calibration

113 The natural way of addressing the problem of overflow or underflow during computation of Layer-
 114 Norm would be to appropriately scale its input. Determining the correct scaling factors appears to
 115 be challenging because while avoiding overflow we also do not want to excessively dump the input
 116 causing underflow and vice versa. As a consequence, any reasonable scaling algorithm must take
 117 into account the actual LayerNorm input values and cannot set the scaling parameters blindly.

118 A common solution would be to calibrate the scaling factors. This involves passing a test dataset
 119 through the Transformer to gauge the range of the input vector norms and setting the scaling factor
 120 based on some first-order statistic of this range (e.g., mean or median norm). This technique requires
 121 extra calibration data and significant computational overhead even for such a basic operation as
 122 LayerNorm, making this approach impractical.

123 3.2 Analytical Static Scaling

124 In this work, we propose a different methodology that enables analytical offline computation of the
 125 desired scaling factors. The scales are determined solely based on the static weights of the liner
 126 layers immediately preceding the LayerNorm at hand. This way we calibrate all the LayerNorm
 127 operators of a model statically, without using a calibration dataset or additional runtime resources
 128 — everything is computed preemptively during model compilation.

129 The idea of the method is based on a simple observation that LayerNorms inside a Transformer oc-
 130 cur frequently and in a regular pattern since any large Transformer is a chain of dozens of identical
 131 decoders. Typically, two consecutive LayerNorms surround the attention or the Multi-Layer Percep-
 132 tron (MLP) block of every decoder. Eq. 1 suggests that we can treat a LayerNorm as a Euclidean

133 normalization followed by a diagonal matrix multiplication.¹ From this natural decomposition of the
 134 LayerNorm operator we infer that immediately after normalization (the first step in LayerNorm), the
 135 norm of the hidden vector \mathbf{x} is equal to one. Our goal is to trace the computational graph from this
 136 point to the next LayerNorm and gauge the orders of magnitude of $\|\mathbf{x}\|$ changes based on the trans-
 137 formations it undergoes along the way.

138 3.3 SLaNC for Standard MLP Block

139 To illustrate the idea, let us consider the MLP block of a standard Transformer, Fig. 2a. Since we
 140 neglect the additive bias β , the output of the MLP block can be expressed as

$$\mathbf{y} = \mathcal{F}(\mathbf{x}\Gamma\mathbf{E})\mathbf{G} + \mathbf{x}\Gamma, \quad (3)$$

141 where the addition comes from the residual connection, and $\mathcal{F}(\cdot)$ is an element-wise non-linearity
 142 which is usually a contraction function (e.g. ReLU, GeLU, etc.) making the norm of its argument
 143 smaller. Since usually, the maximal partial derivative of $\mathcal{F}(\cdot)$ is bounded by a constant close to one,
 144 we can approximate the norm of \mathbf{y} as

$$\|\mathbf{y}\| \propto \|\mathbf{x}\Gamma\mathbf{E}\mathbf{G} + \mathbf{x}\Gamma\|_F. \quad (4)$$

145 Eventually, we conclude that

$$\frac{\|\mathbf{y}\|}{\|\mathbf{x}\|} \propto \|\Gamma(\mathbf{E}\mathbf{G} + \mathbf{I})\|_F. \quad (5)$$

146 Recall that \mathbf{x} is the output of the normalization step of a LayerNorm (see Fig. 2a) and thus has unit
 147 norm. Therefore, it is natural to set the scaling factor of the following LayerNorm to the right-hand
 148 side of Eq. 5 and this should solve the overflow/underflow issue. In Section 4, we demonstrate by
 149 extensive simulations that this is actually the case. Note that the scale determined by Eq. 5 only
 150 involves static weights and can be computed offline.

151 3.4 SLaNC for Llama MLP Block

152 Using the same methodology, we derive an analogous formula for the scaling factors of the Layer-
 153 Norm following the modified MLP block designed for the decoders of the Llama family of models,
 154 Fig. 2b. Here, in addition to the two linear layers of the standard MLP block, we have another
 155 linear layer whose output is multiplied with the output of the non-linearity in the element-wise man-
 156 ner. The non-linear function itself is usually chosen to be GeLU. The input of the post-MLP block
 157 LayerNorm \mathbf{y} reads as

$$\mathbf{y} = (\mathcal{F}(\mathbf{x}\Gamma\mathbf{E}) \odot \mathbf{x}\Gamma\mathbf{B})\mathbf{G} + \mathbf{x}\Gamma. \quad (6)$$

158 Similar principles as above together with basic properties of matrix norms yield

$$\|\mathbf{y}\| \propto \|\|\Gamma\mathbf{E}\|\mathbf{x}\Gamma\mathbf{B}\mathbf{G} + \mathbf{x}\Gamma\|_F, \quad (7)$$

159 where we used the fact that $\|\mathbf{x}\| = 1$. Finally, the scaling factor computes as

$$\frac{\|\mathbf{y}\|}{\|\mathbf{x}\|} \propto \|\Gamma(\|\Gamma\mathbf{E}\|\mathbf{B}\mathbf{G} + \mathbf{I})\|_F. \quad (8)$$

160 3.5 SLaNC for the Attention Block

161 Next, we derive a formula for the scaling factor of the LayerNorm following the standard attention
 162 block with h heads. As it can be seen in Fig. 2c, the most critical observation here is that the product
 163 of the Softmax output \mathbf{S}^i of head i with \mathbf{V}^i results in a convex combination of the rows of the
 164 latter. The outputs $\{\mathbf{S}^i\mathbf{V}^i\}_{i=1}^h$ are concatenated, hence, the norm of the concatenated vector can be
 165 approximated by the norm of the concatenation of $\{\mathbf{x}\Gamma\mathbf{W}_{\mathbf{V}}^i\}_{i=1}^h$ which is precisely $\mathbf{x}\Gamma\mathbf{W}_{\mathbf{V}}$. We get

$$\|\mathbf{y}\| \propto \|\mathbf{x}\Gamma\mathbf{W}_{\mathbf{V}}\mathbf{P} + \mathbf{x}\Gamma\|_F = \|\mathbf{x}\Gamma(\mathbf{W}_{\mathbf{V}}\mathbf{P} + \mathbf{I})\|_F, \quad (9)$$

166 and conclude that the following scale should be used in the post-attention LayerNorm operator

$$\frac{\|\mathbf{y}\|}{\|\mathbf{x}\|} \propto \|\Gamma(\mathbf{W}_{\mathbf{V}}\mathbf{P} + \mathbf{I})\|_F. \quad (10)$$

¹Since we are mainly focusing on the order of magnitude of the norms of the hidden states involved, without impact on accuracy we discard the additive biases β of the LayerNorm operator.

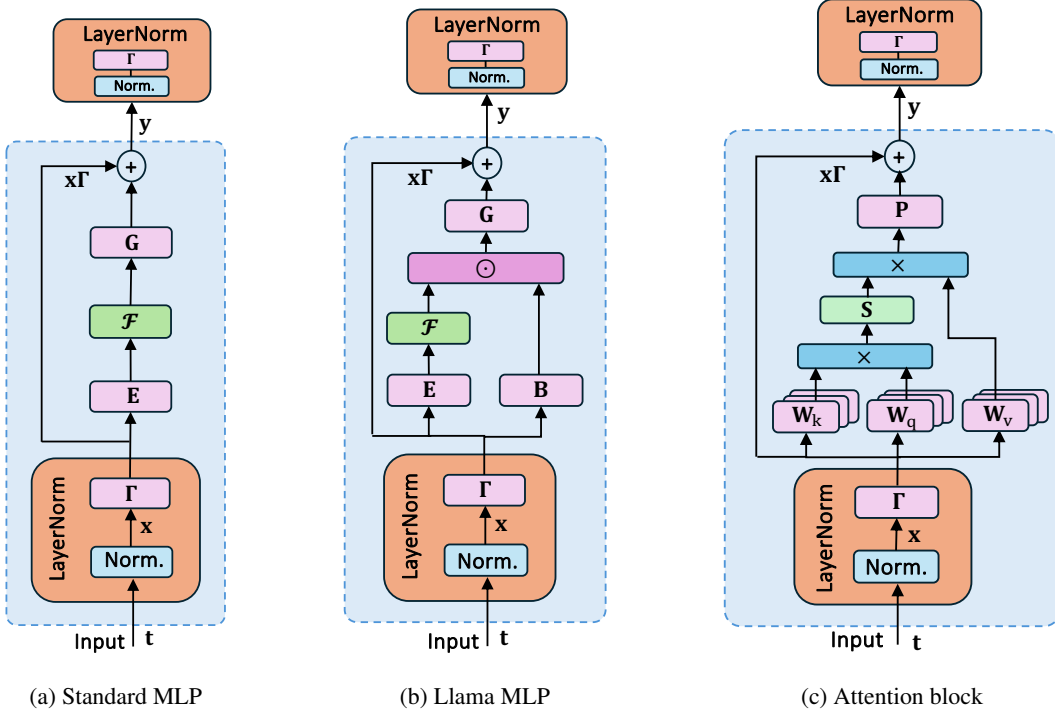


Figure 2: The compute flow between consecutive LayerNorms of various Transformers. Pink blocks with capital letters stand for linear layers with the corresponding weight matrices, green \mathcal{F} -blocks represent non-linearities and \mathcal{S} -block represents Softmax.

167 **4 Experiments**

168 To demonstrate the power of our SLaNC scaling technique, we present simulation results for Llama
 169 models. Note that the Llama architecture replaces the LayerNorm by Root Mean Squared Layer
 170 Normalization (RMSNorm) [35], which differs from the former only by omitting the mean μ sub-
 171 traction in Eq. 2 and thus does not affect SLaNC scaling.

172 In our first experiment, we collected empirical statistics of the sums of squares in the denominators
 173 of the RMSNorm operators without scaling and with SLaNC scaling. To this end, we applied Llama-
 174 2-7b to Wikitext 2 dataset. Fig. 3a and 3c feature typical histograms in two consecutive RMSNorms
 175 of this model. We see that in a significant number of cases, the sum of squares well exceeds the
 176 FP16 range and causes overflow. The SLaNC scaling changes the situation dramatically and not
 177 only shifts the histograms inside the FP16 range but also keeps safe margins on both edges of the
 178 range, as illustrated by Fig. 3b and 3d, respectively.

179 Next, we compared the perplexities of Llama models on the same Wikitext 2 dataset with the default
 180 FP32 implementation of RMSNorm and with the sum of squared accumulated in FP16 (all other
 181 operations from the default setup intact). Table 1 shows a significant degradation when the accu-
 182 mulation happens in FP16 exactly due to numerous overflows. This problem is completely resolved
 183 when the SLaNC scaling is applied. We also note that in all standard models, a small constant ε is
 184 added to the variance of the input in the denominator of LayerNorm or RMSNorm operator. This
 185 way we can avoid division by zero in the case of underflow and improve the numerical stability.
 186 Since SLaNC scales are known ahead of time, we can easily apply them to the ε constants as well
 187 (in fact, we divide ε by the squared SLaNC scalings). As the bottom row of Table 1 demonstrates,
 188 now the FP16 SLaNC scaling can precisely reproduce the default FP32 values.

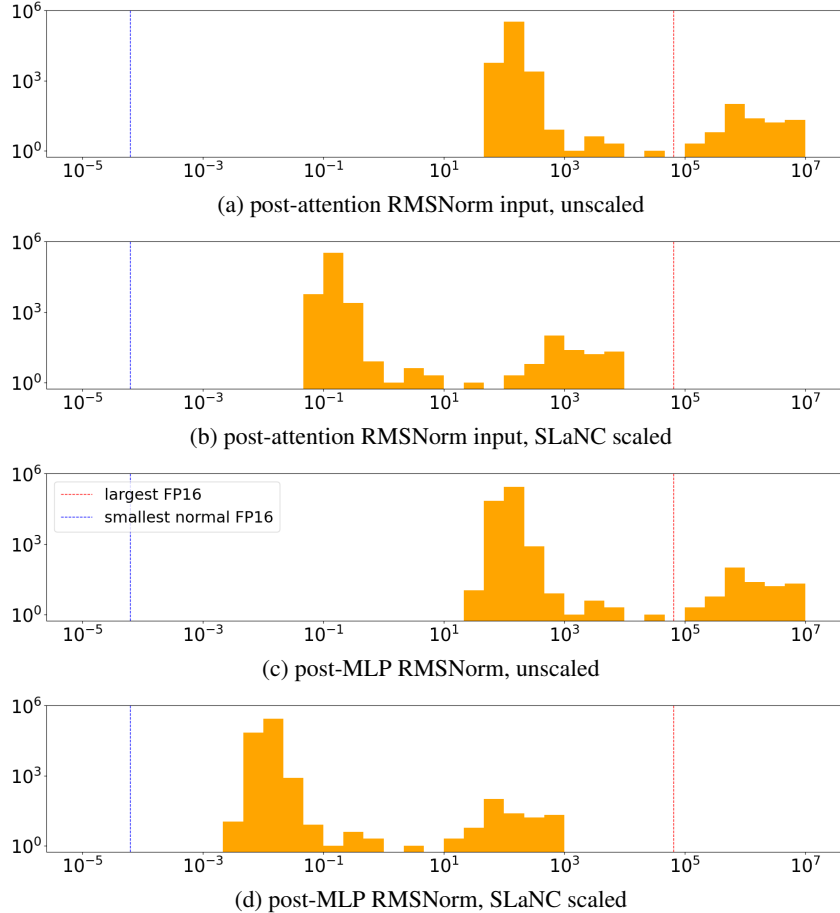


Figure 3: Empirical histograms of the sum of squares in RMSNorm layers of the 9th decoder in Llama-2-7b, calculated on wikitext2. The red vertical cut-off line sets the maximal representable FP16 value (65k) beyond which FP16 overflows, the blue line shows the minimal normal FP16 value. Histograms (b) and (d) show that after SLaNC scaling no overflow (or underflow) is detected and the RMSNorm is computed precisely.

Table 1: Llama perplexity on Wikitext 2 with different RMSNorm computation modes.

accumulation format	Llama-2-7b	Llama-2-13b	Llama-3-8b
FP32	5.116	4.574	5.538
FP16	19.105	10.521	16.013
FP16 + SLaNC	5.116	4.573	5.539

189 5 Conclusion

190 In this paper, we present a novel SLaNC technique that makes LLM inference possible on FP16
 191 accelerators without the need to cast LayerNorm operators into FP32. This theoretically grounded
 192 approach provides easy-to-use formulae for an offline computation of scaling factors for the inputs of
 193 LayerNorms. The SLaNC scaling factors guarantee precise computation of the LayerNorm in FP16
 194 and provably avoid overflows and underflows. By keeping all the compute in FP16, the SLaNC
 195 algorithm enables low latency accurate compute, which is demonstrated by our extensive numerical
 196 simulations.

197 **References**

- 198 [1] Ashish Vaswani, Noam Shazeer, Niki Parmar, Jakob Uszkoreit, Llion Jones, Aidan N Gomez,
199 Łukasz Kaiser, and Illia Polosukhin. Attention is all you need. In *Advances in Neural Infor-*
200 *mation Processing Systems*, pages 5998–6008, 2017.
- 201 [2] Jacob Devlin, Ming-Wei Chang, Kenton Lee, and Kristina Toutanova. BERT: Pre-training of
202 deep bidirectional Transformers for language understanding. In *North American Chapter of*
203 *the Association for Computational Linguistics*, 2019.
- 204 [3] Zihang Dai, Zhilin Yang, Yiming Yang, Jaime G. Carbonell, Quoc V. Le, and Ruslan Salakhut-
205 dinov. Transformer-XL: Attentive language models beyond a fixed-length context. In *Annual*
206 *Meeting of the Association for Computational Linguistics*, 2019.
- 207 [4] Yinhan Liu, Myle Ott, Naman Goyal, Jingfei Du, Mandar Joshi, Danqi Chen, Omer Levy,
208 Mike Lewis, Luke Zettlemoyer, and Veselin Stoyanov. RoBERTa: A robustly optimized BERT
209 pretraining approach. *arXiv preprint arXiv:1907.11692*, 2019.
- 210 [5] Alexey Dosovitskiy, Lucas Beyer, Alexander Kolesnikov, Dirk Weissenborn, Xiaohua Zhai,
211 Thomas Unterthiner, Mostafa Dehghani, Matthias Minderer, Georg Heigold, Sylvain Gelly,
212 Jakob Uszkoreit, and Neil Houlsby. An image is worth 16x16 words: Transformers for image
213 recognition at scale. In *International Conference on Learning Representations*, 2021.
- 214 [6] Amir Gholami, Sehoon Kim, Zhen Dong, Zhewei Yao, Michael W Mahoney, and Kurt Keutzer.
215 A survey of quantization methods for efficient neural network inference. In *Low-Power Com-*
216 *puter Vision*, pages 291–326. Chapman and Hall/CRC, 2022.
- 217 [7] Xindi Wang, Mahsa Salmani, Parsa Omid, Xiangyu Ren, Mehdi Rezagholizadeh, and Ar-
218 maghan Eshaghi. Beyond the limits: A survey of techniques to extend the context length in
219 large language models. *arXiv preprint arXiv:2402.02244*, 2024.
- 220 [8] Bitar Darvish Rouhani, Daniel Lo, Ritchie Zhao, Ming Liu, Jeremy Fowers, Kalin Ovtcharov,
221 Anna Vinogradsky, Sarah Massengill, Lita Yang, Ray Bittner, Alessandro Forin, Haishan Zhu,
222 Taesik Na, Prerak Patel, Shuai Che, Lok Chand Koppaka, XIA SONG, Subhojit Som, Kaustav
223 Das, Saurabh T, Steve Reinhardt, Sitaram Lanka, Eric Chung, and Doug Burger. Pushing
224 the limits of narrow precision inferencing at cloud scale with Microsoft floating point. In
225 H. Larochelle, M. Ranzato, R. Hadsell, M.F. Balcan, and H. Lin, editors, *Advances in Neural*
226 *Information Processing Systems*, volume 33, pages 10271–10281. Curran Associates, Inc.,
227 2020.
- 228 [9] Bitar Darvish Rouhani, Ritchie Zhao, Ankit More, Mathew Hall, Alireza Khodamoradi, Sum-
229 mer Deng, Dhruv Choudhary, Marius Cornea, Eric Dellinger, Kristof Denolf, et al. Microscal-
230 ing data formats for deep learning. *arXiv preprint arXiv:2310.10537*, 2023.
- 231 [10] Ilya Soloveychik, Ilya Lyubomirsky, Xin Wang, and Sudeep Bhoja. Block format error bounds
232 and optimal block size selection. *AAAI Conference, ENC2 workshop*, 2023.
- 233 [11] Zhewei Yao, Reza Yazdani Aminabadi, Minjia Zhang, Xiaoxia Wu, Conglong Li, and Yuxiong
234 He. ZeroQuant: Efficient and affordable post-training quantization for large-scale Transform-
235 ers. *Advances in Neural Information Processing Systems*, 35:27168–27183, 2022.
- 236 [12] Elias Frantar and Dan Alistarh. SparseGPT: Massive language models can be accurately
237 pruned in one-shot. In *International Conference on Machine Learning*, pages 10323–10337.
238 PMLR, 2023.
- 239 [13] Krzysztof Choromanski, Valerii Likhoshesterov, David Dohan, Xingyou Song, Andreea Gane,
240 Tamas Sarlos, Peter Hawkins, Jared Davis, Afroz Mohiuddin, Łukasz Kaiser, et al. Rethinking
241 attention with performers. *arXiv preprint arXiv:2009.14794*, 2020.
- 242 [14] Sinong Wang, Belinda Z Li, Madian Khabsa, Han Fang, and Hao Ma. Linformer: Self-
243 attention with linear complexity. *arXiv preprint arXiv:2006.04768*, 2020.

- 244 [15] Zhen Qin, Weixuan Sun, Hui Deng, Dongxu Li, Yunshen Wei, Baohong Lv, Junjie Yan, Ling-
245 peng Kong, and Yiran Zhong. cosformer: Rethinking softmax in attention. *arXiv preprint*
246 *arXiv:2202.08791*, 2022.
- 247 [16] Elias Frantar, Saleh Ashkboos, Torsten Hoefer, and Dan Alistarh. GPTQ: Accu-
248 rate post-training quantization for generative pre-trained Transformers. *arXiv preprint*
249 *arXiv:2210.17323*, 2022.
- 250 [17] Ji Lin, Jiaming Tang, Haotian Tang, Shang Yang, Wei-Ming Chen, Wei-Chen Wang, Guangx-
251 uan Xiao, Xingyu Dang, Chuang Gan, and Song Han. AWQ: Activation-aware weight quan-
252 tization for on-device LLM compression and acceleration. *Proceedings of Machine Learning*
253 *and Systems*, 6:87–100, 2024.
- 254 [18] Guangxuan Xiao, Ji Lin, Mickael Seznec, Hao Wu, Julien Demouth, and Song Han.
255 SmoothQuant: Accurate and efficient post-training quantization for large language models.
256 In *International Conference on Machine Learning*, pages 38087–38099. PMLR, 2023.
- 257 [19] Coleman Hooper, Sehoon Kim, Hiva Mohammadzadeh, Michael W Mahoney, Yakun Sophia
258 Shao, Kurt Keutzer, and Amir Gholami. KVQuant: Towards 10 million context length LLM
259 inference with KV cache quantization. *arXiv preprint arXiv:2401.18079*, 2024.
- 260 [20] Nikita Trukhanov and Ilya Soloveychik. Accurate block quantization in LLMs with outliers.
261 *AAAI Conference, ENC2 Workshop*, 2024.
- 262 [21] Bitar Darvish Rouhani, Ritchie Zhao, Venmugil Elango, Rasoul Shafipour, Mathew Hall, Maral
263 Mesmakhosroshahi, Ankit More, Levi Melnick, Maximilian Golub, Girish Varatkar, et al. With
264 shared microexponents, a little shifting goes a long way. In *Proceedings of the 50th Annual*
265 *International Symposium on Computer Architecture*, pages 1–13, 2023.
- 266 [22] Paulius Micikevicius, Sharan Narang, Jonah Alben, Gregory Diamos, Erich Elsen, David Gar-
267 cia, Boris Ginsburg, Michael Houston, Oleksii Kuchaiev, Ganesh Venkatesh, and Hao Wu.
268 Mixed precision training. In *International Conference on Learning Representations*, 2018.
- 269 [23] Swagath Venkataramani, Vijayalakshmi Srinivasan, Wei Wang, Sanchari Sen, Jintao Zhang,
270 Ankur Agrawal, Monodeep Kar, Shubham Jain, Alberto Mannari, Hoang Tran, Yulong Li,
271 Eri Ogawa, Kazuaki Ishizaki, Hiroshi Inoue, Marcel Schaal, Mauricio Serrano, Jungwook
272 Choi, Xiao Sun, Naigang Wang, Chia-Yu Chen, Allison Allain, James Bonano, Nianzheng
273 Cao, Robert Casatuta, Matthew Cohen, Bruce Fleischer, Michael Guillorn, Howard Haynie,
274 Jinwook Jung, Mingu Kang, Kyu-hyoun Kim, Siyu Koswatta, Saekyu Lee, Martin Lutz, Sil-
275 via Mueller, Jinwook Oh, Ashish Ranjan, Zhibin Ren, Scot Rider, Kerstin Schelm, Michael
276 Scheuermann, Joel Silberman, Jie Yang, Vidhi Zalani, Xin Zhang, Ching Zhou, Matt Ziegler,
277 Vinay Shah, Moriyoshi Ohara, Pong-Fei Lu, Brian Curran, Sunil Shukla, Leland Chang, and
278 Kailash Gopalakrishnan. RaPiD: AI accelerator for ultra-low precision training and inference.
279 In *2021 ACM/IEEE 48th Annual International Symposium on Computer Architecture (ISCA)*,
280 pages 153–166, 2021.
- 281 [24] Norman P Jouppi, Cliff Young, Nishant Patil, David Patterson, Gaurav Agrawal, Raminder
282 Bajwa, Sarah Bates, Suresh Bhatia, Nan Boden, Al Borchers, et al. In-datacenter performance
283 analysis of a tensor processing unit. In *Proceedings of the 44th Annual International Sympo-*
284 *sium on Computer Architecture*, pages 1–12, 2017.
- 285 [25] Shaked Brody, Uri Alon, and Eran Yahav. On the expressivity role of layernorm in Transform-
286 ers’ attention. In *Annual Meeting of the Association for Computational Linguistics*, 2023.
- 287 [26] Jialong Guo, Xinghao Chen, Yehui Tang, and Yunhe Wang. SLAB: Efficient Transformers
288 with simplified linear attention and progressive re-parameterized batch normalization. *arXiv*
289 *preprint arXiv:2405.11582*, 2024.
- 290 [27] Yelysei Bondarenko, Markus Nagel, and Tijmen Blankevoort. Understanding and overcoming
291 the challenges of efficient Transformer quantization. *ArXiv*, abs/2109.12948, 2021.
- 292 [28] Markus Nagel, Marios Fournarakis, Rana Ali Amjad, Yelysei Bondarenko, Mart Van Baalen,
293 and Tijmen Blankevoort. A white paper on neural network quantization. *arXiv preprint*
294 *arXiv:2106.08295*, 2021.

- 295 [29] Jimmy Ba, Jamie Ryan Kiros, and Geoffrey E Hinton. Layer normalization. *arXiv preprint*
296 *arXiv:1607.06450*, 2016.
- 297 [30] Sergey Ioffe and Christian Szegedy. Batch normalization: Accelerating deep network training
298 by reducing internal covariate shift. In *Proceedings of the 32nd International Conference*
299 *on International Conference on Machine Learning - Volume 37*, ICML'15, page 448–456.
300 JMLR.org, 2015.
- 301 [31] Yuxin Wu and Kaiming He. Group normalization. In *Proceedings of the European Conference*
302 *on Computer Vision (ECCV)*, pages 3–19, 2018.
- 303 [32] Stefano Markidis, Steven Wei Der Chien, Erwin Laure, Ivy Bo Peng, and Jeffrey S Vetter.
304 NVIDIA tensor core programmability, performance & precision. In *2018 IEEE International*
305 *Parallel and Distributed Processing Symposium Workshops (IPDPSW)*, pages 522–531. IEEE,
306 2018.
- 307 [33] Dheevatsa Mudigere, Yuchen Hao, Jianyu Huang, Zhihao Jia, Andrew Tulloch, Srinivas Srid-
308 haran, Xing Liu, Mustafa Ozdal, Jade Nie, Jongsoo Park, et al. Software-hardware co-design
309 for fast and scalable training of deep learning recommendation models. In *Proceedings of the*
310 *49th Annual International Symposium on Computer Architecture*, pages 993–1011, 2022.
- 311 [34] Ruibin Xiong, Yunchang Yang, Di He, Kai Zheng, Shuxin Zheng, Chen Xing, Huishuai Zhang,
312 Yanyan Lan, Liwei Wang, and Tieyan Liu. On layer normalization in the Transformer archi-
313 tecture. In *International Conference on Machine Learning*, pages 10524–10533. PMLR, 2020.
- 314 [35] Biao Zhang and Rico Sennrich. Root mean square layer normalization. *arXiv preprint*
315 *arXiv:1910.07467*, 2019.